A Control Strategy for Ground Source Heat Pump Performance Optimization with a Non-homogeneous Soil Profile

Amir Rezaei-Bazkiaei[1,*], Ehsan Dehghan-Niri[3], Gary F. Dargush[2], A. Scott Weber[1]

Abstract

An effective control strategy with a non-homogeneous soil profile for horizontal Ground Source Heat Pumps (GSHPs) was investigated in this paper. Steps toward development of a comprehensive model to consider the effects of an intermediate blanket overlaying the ground pipes were described. The model incorporates the effects of a variety of surface energy fluxes to provide an accurate estimate of the ground thermal regime. The developed model was utilized successfully in conjunction with the Genetic Algorithm (GA) evolutionary search algorithm to obtain the optimized operational parameters for a GSHP in three different climate conditions. A properly sized and engineered non-homogeneous soil profile demonstrated the potential to boost the capacity of GSHP systems to a significant level. The potential benefits of a recycled product, Tire Derived Aggregate (TDA), as an insulation blanket was assessed via the optimization algorithm. TDA was demonstrated to be more effective in the heating mode in a cold climate (Buffalo) by increasing the energy extraction rates from the ground by about approximately 15 % annually. TDA's effectiveness was less pronounced in a relatively moderate climate (Dallas) for heating purposes with efficiency improvements of about 4 % annually. The annual percentage increase in efficiency for cooling season with TDA blanket was higher for Buffalo (7.6 %) compared to Dallas (3.5 %). For the cooling only purposes (Miami), a high conductive intermediate layer (saturated clay) exhibited greater potential to enhance the efficiency in coldest months in a warm climate. The results are highly suggestive of the beneficial application of a layered system to increase the performance of GSHPs. A shift in design approach toward consideration of more control strategies for the ground pipe side of GSHPs is suggested based on the model results. A field demonstration project with TDA blanket has been constructed at the University at Buffalo to further investigate the findings with regard to field conditions and other characteristics of TDA material.

Keywords: Ground source heat pump, tire derived aggregate, non-homogeneous, optimization, genetic algorithm, energy efficiency, control

1. Introduction

Every ground source heat pump (GSHP) consists of two main parts; the ground side and the heat pump inside the building. The ground side, also referred to as the heat source/sink, consists of the ground pipe network and the

☆Corresponding author's address: 204 Jarvis Hall, University at Buffalo, Buffalo, NY, 14260. Tel: (716) 380-5255. Fax: (716) 645-3667
  Email addresses: ar92@buffalo.edu (Amir Rezaei-Bazkiaei), ehsandeh@buffalo.edu (Ehsan Dehghan-Niri), gdargush@buffalo.edu (Gary F. Dargush), sweber@buffalo.edu (A. Scott Weber)
  [1]Department of Civil , Structural & Environmental Engineering, University at Buffalo, Buffalo, NY-14260
  [2]Department of Mechanical & Aerospace Engineering, University at Buffalo, Buffalo, NY-14260
  [3]Smart Structures Research Lab, Department of Civil, Structural & Environmental Engineering, University at Buffalo, NY 14260

circulating pump. The heat pump unit itself consists of sub-units which handle the thermodynamic relationships between the working fluid and the load side (indoor air or indoor water network); compressor, condenser, evaporator, the expansion device and/or blower fans or circulating indoor water pumps. The working fluid flows through the ground pipes and exchanges heat with the surrounding soil medium where it gains/loses heat in heating/cooling modes respectively. The fluid at the outlet of the pipe enters the heat pump where the thermodynamic cycle of the heat exchange between the working fluid and the refrigerant is responsible for heat delivery or dissipation in heating and cooling modes respectively. A successful design of GSHP involves careful selection and sizing of both the ground side and the indoor unit so that heating/cooling loads are met year-round with least waste heat/electricity inventory. This selection process usually involves employment of simplifying engineering assumptions. For example, one of the most well-known ground pipe sizing semi-empirical formulas is based on the concept of thermal resistance calculation for the soil, pipe and working fluid [1]. Resistance factor calculation is based on the line source theory which assumes a constant source of heat propagates continuously through the soil medium of interest. An assumption which is not a real representative of the ground pipe operation but is assumed to be within reasonable range of error for an engineering practice.

The heat pump sizing starts with the careful estimation of the heating/cooling loads for the prospect building via accepted methods such as the bin method. The bin method is based on a full survey of the total number of hours in a design year that a certain air temperature range (bin) occurs. The heating/cooling budget analysis forms the base for the peak load GSHP design. It is noteworthy that methods like bin method do not take into account the sequence or real-time occurrence of the peak load demand in time. In other words, the question is the duration of a worst case load condition rather than when and for how long the load sustain. Therefore, it does not matter in such design procedures what is the climate and/or source condition before and after the worst case condition, a matter that can influence the overall performance of the system. Moreover, these methods usually assume a constant source/sink strength (ground temperature) based on the maximum and minimum observed data or semi-experimental formulas [1] which again does not reflect on the dynamic variation of the boundary conditions and the time dependent nature of the system's functionality. Inherent tendency of the traditional design methods like this to stray from the path of optimized operation has made the dynamic, real-time analysis of GSHPs the focus of many recent research works [2, 3]. The following design steps after the heat budget analysis involve ground pipe sizing and heat pump selection.

One of the most essential parts of a GSHP design, after a meticulous selection of the pipe length and size, is the proper selection of the working fluid temperature range that enters the ground. International ground source heat pump association (IGSHPA) suggests an equation mainly based on experiment (equation 1) which relates the inlet water temperature to the heat pump to maximum, minimum and average ambient air temperatures. It is the responsibility of the designer to select the appropriate optimal entering water temperature to the heat pump that guarantees efficient performance. Given the complexities of an accurate building load demand evaluation (users consumption habits, level of building insulation, changes in occupancy, and specially sudden climatic changes which are far different from the long term statistical design year data, etc.) and its causal relationship with the GSHP system units, the optimization of the overall performance of a GSHP becomes a real challenge. Add to the problem, the ground characteristics variation in different regions to make it even more challenging to track the dynamic building load demand and keep the heating/conditioning process as optimized as possible. This paper aims to help designers of GSHPs achieve optimal design specifications by utilization of an evolutionary optimization algorithm. The central motive behind this research is to obtain optimized values for the functional parameters of a GSHP system which can be applied practically via employment of control measures such as variable refrigerant flow heat pumps.

With the ever increasing need for preserving energy, the idea of utilization of capacity control strategies for GSHPs was initiated by researchers about two decades ago [4]. The capacity control practices in their core deal with the most feasible engineering options to dynamically meet the building load requirements and minimize the waste energy in the heating/conditioning process. As Madani summarizes [5], capacity control usually involves either the control on the components of a GSHP system (e.g. the compressor, condenser, ground pipes, etc.) or a change in design configurations for different seasons or advanced control algorithms. The complex nature of the interplay of relationships between the units of a GSHP is in such a way that changes in operational parameters of one unit can affect the overall performance of the system. From the modeling point of view, researchers have tried to tackle these complexities by dynamically modeling the interactions between these units via packaged softwares such as TRNSYS [6, 7, 8, 9, 10, 2] or in combination with thermodynamic data base models such as EES [3] or by self developed programs [11] which are capable of modeling the dynamic between these units. The general structure of such modeling efforts often consists of separate first-level models (e.g. ground pipe and heat pump) which each have sub-models of second-level (e.g. compressor, evaporator, etc.) with higher details. The functional relationship between the sub-models is constructed via operational parameters such as water/brine and refrigerant flow rates. The level of complexity of these sub-models significantly depends on the purpose of the modeling effort as Madani [5] describes.

Despite numerous efforts to impose control measures on the heat pump side of a GSHP system, there has been put little thoughts into the potential of having control on the ground characteristics. This is perhaps because of a predisposition to believe that ground related works usually are associated with extra capital investment that makes any modification less favorable than making changes to the heat pump unit. Our findings [12] suggest that utilization of a layered system above the pipe burial depth might be worth more attention. The layered system demonstrated the potential to increase the energy extraction rates from the ground to about 17 %, in the peak heating month, compared to the homogeneous case with the local soil profile. This paper aims at assessing the effectiveness of a non-homogeneous soil profile for different climate conditions by obtaining the optimized functional parameters for these different climates.

Our focus in this paper is mainly on the analysis of the system efficiency and optimization via control on the source/sink (ground) side with an eye on the heat pump unit. A simple semi-empirical equation (1) for the entering water temperature to the pump was adopted from the international ground source heat pump association (IGSHPA) design manual [1] to make the link between the ground pipe and the heat pump. The ground pipe model, on the other hand, is an elaborate version of a surface energy balance model which unlike thermal resistance method is capable of solving for the temperature distribution of the entire soil profile in order to obtain the outlet water temperature from the ground pipes. A detailed description of the surface energy balance equations, parameters and the solution methods is presented in [12]. A summary of the heat fluxes is listed in the 'surface energies' section. Our motivation behind development of such ground model arises from the desire to investigate the potential benefits of a non-homogeneous soil profile on the ground pipe performance. The developed model was employed to investigate the effectiveness of utilization of a recycled product of tire industry as an insulation material above the burial depth of the ground pipes.

$$EWT_h = EWT_{min} + \frac{EWT_{mean} - EWT_{min}}{T_{airmean} - T_{airmin}} \left(T_{air} - T_{airmax}\right)$$

(1)

$$EWT_c = EWT_{mean} + \frac{EWT_{max} - EWT_{mean}}{T_{airmax} - T_{airmean}} \left(T_{air} - T_{airmean}\right)$$

where: EWT_h: entering water temperature in heating mode, EWT_c: entering water temperature in cooling mode, EWT_{min}: minimum design entering water temperature, EWT_{mean}: average design entering water temperature, EWT_{max}: maximum design entering water temperature, $T_{airmean}$: average annual ambient air temperature, T_{airmin}: minimum annual ambient air temperature, T_{airmax}: maximum annual ambient air temperature, T_{air}: air temperature at the time of simulation

Tire Derived Aggregate (TDA) is the proposed insulation material to be used as the intermediate layer in the non-homogeneous model. TDA mainly consists of chopped pieces of used tires in a variety of nominal sizes ranging from 1 to above 5 inches [13]. The idea of production of TDA from used tires, also referred to as tire chips, tire shreds, and tire mulch, was first initiated by Humphrey [14]. New applications for TDA, mostly in civil engineering, were proposed based on its unique physical characteristics. TDA's relatively low density compared to conventional backfill makes it a viable alternative fill material where a lighter fill material is desired in construction works [15]. Its low thermal conductivity on the other hand, provoked the thought of utilizing TDA as an alternative insulation material in road base insulation and some agricultural applications to modulate temperature fluctuation on the soil surface [14, 13, 16]. There are only a few studies in the literature that focus on the properties of TDA measuring physical properties [16], compaction densities for different sizes of chips [13] and also thermal properties of tire chip samples [13, 17, 18]. A list of thermal properties and density of tire shreds reported in these studies is presented in Table 1. A thermal conductivity value of 0.29 $Wm^{-1\circ}C^{-1}$, specific heat of 500 $JKg^{-1\circ}C^{-1}$ and density of 720 Kgm^{-3} were chosen as representative properties of TDA material for the purpose of the analyses in this paper.

Table 1: TDA thermal and physical properties in literature

Reference	Material	Thermal conductivity ($Wm^{-1\circ}C^{-1}$)	Specific heat ($JKg^{-1\circ}C^{-1}$)	Density (Kgm^{-3})
Wappet (2006)	Tire shred	0.564	507	641
Shao (1995)	Tire chips	0.149-0.164	NA	513
Humphrey (2002)	Tire chips	0.29	1.15	720
Moo-young (2003)	Tire chips	NA	NA	1060-1100

In the following sections, the development of a model for horizontal ground pipes in a non-homogeneous soil profile was described first. The model was then used in conjunction with the developed genetic algorithm optimization model to search for the optimized operational parameters of the GSHP. The optimization was carried out for same pipe characteristics and different cities across United States to evaluate the effects of climatic conditions on the select optimized parameters. Detailed description of the methods and results are presented in the following sections.

2. Material and methods

A brief summary of the surface energy balance equations are first introduced. The second subsection describes the ground pipe specifications and also the way pipes are modeled from the physical domain into the numerical domain. Numerical solution of the ground pipe model and the parameter settings for the genetic algorithm are described in the following sections.

2.1. Surface energies

The surface boundary condition takes into account the effects of energy balance due to variety of mechanisms responsible for surface-ambient heat interaction. The total energy balance on the ground surface (Q_t, $Watts$) can be written as [19, 20]:

$$Q_t = Q_c + Q_e + Q_h + Q_{le} + Q_{li} + Q_{si} + Q_p \qquad (2)$$

Q_c= Conduction heat flux through snow layer or ground surface (Watts)

Q_e= Turbulent exchange of latent heat (Watts)

Q_h= Turbulent exchange of sensible heat (Watts)

Q_{le}= Emitted long wave radiation heat flux (Watts)

Q_{li}= Incoming long wave radiation (Watts)

Q_{si}= Solar radiation reaching the surface of earth (Watts)

Q_p= Heat flux due to precipitation (Watts)

For a detailed description of each heat flux input parameters and formulas refer to [12].

2.2. Ground pipe modeling

The ground pipes configuration consists of a horizontal pipe of total length of 61 meters (L) and $\frac{3}{4}$ inch diameter, 3 m distance between inlet and outlet, buried at the depth of 2 m (j_{pipe}), with the working fluid flow rate of 3 gallons per minute (0.19 kg/s). Assuming there is no thermal interaction between pipes, the solution domain (Figure 1) was considered to be from the center line of the pipe to the mid-span of the distance between pipes (1.5 m), in the x-direction, and from ground surface to the farfield (5 m) in the y-direction. Soil thermal conductivity (K_s) and thermal diffusivity (α_s) were selected based on the soil and rock classification guideline [21] to be equal to 1.67 $Wm^{-1\circ}K^{-1}$ and $66 \cdot 10^{-8} \ m^2 s^{-1}$, respectively. For the sake of comparison, this physical setting of the ground pipe was assumed to be the same for other cities in this analysis.

To account for the three-dimensional behavior of the pipe and the surrounding soil, the effect of the working fluid flow rate was considered along the pipe direction. The third dimension of the problem was modeled by splitting the physical domain in the pipe direction into a series of cross sections (slices) of the soil profile for each time step, including the nodal temperature of the fluid at the pipe's location. Figure 2 shows how the slices are spaced in the pipe direction to cover the temperature distribution of the entire 3D domain. At each time step, the nodal temperatures of each cross section were obtained and subsequently updated for the next slice along the pipe's length via equation (4) to achieve a temperature distribution of soil and fluid at the end of the pipe (L). The same process was repeated for the next time steps until the end of the simulation time. A schematic representation of the cross sections is depicted in Figure 1. Detailed description of the numerical schemes and results are described in the following sections.

3. Numerical algorithm

The three-dimensional temperature distribution in the soil media was modeled by solving the governing heat conduction equation and incorporating the heat flow rate forced by the circulating water. The temperature gradient
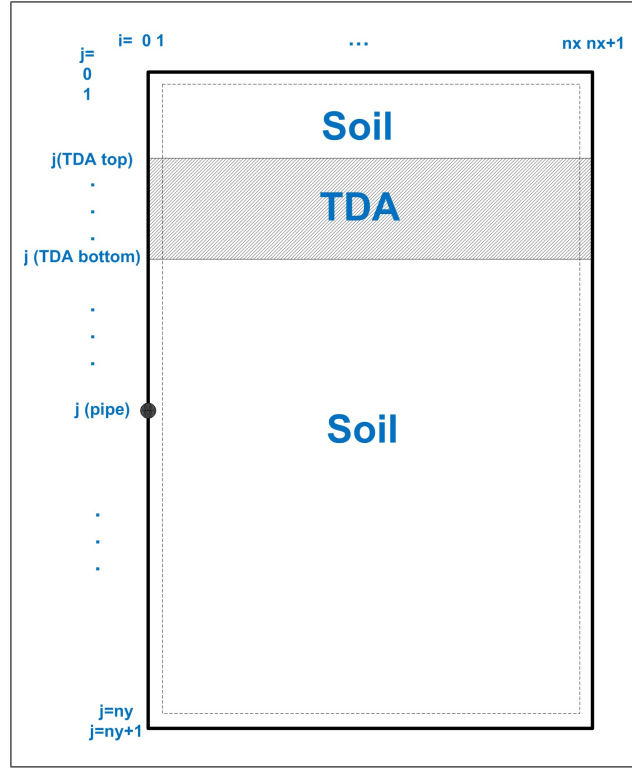
Figure 1: Configuration of pipe, TDA and soil layers, and solution domain discretization [12]
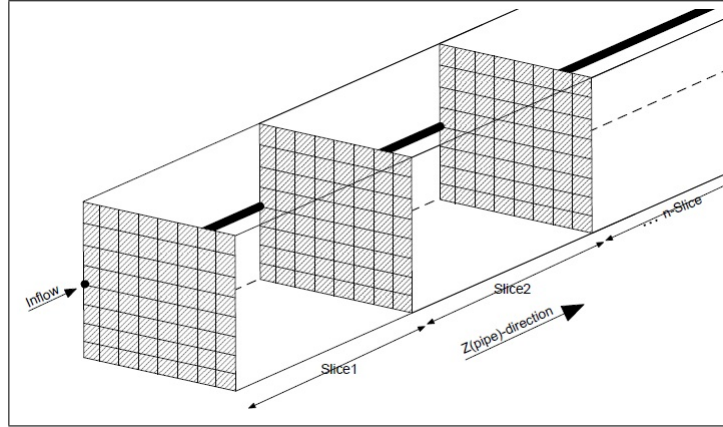

Figure 2: Schematic of slices of 3D domain in pipe directions [12]

in the pipe material is small enough to be neglected allowing the heat equation to be solved in a two-dimensional geometry by inclusion of the fluid temperature in the domain [22]. The governing equation (3) was solved for the entire domain in two-dimensions for the pure heat conduction first, and the solution was then updated along the pipe's length to obtain the solution in three dimensions.

$$\frac{1}{\alpha}\frac{\partial T(x,y,t)}{\partial t} = \frac{\partial^2 T(x,y,t)}{\partial x^2} + \frac{\partial^2 T(x,y,t)}{\partial y^2} \tag{3}$$

The output water temperature equation (4) along the pipe direction, calculated based on the analytical solution for the energy balance between surrounding soil medium and pipe [23], constructs the link between the fluid and the soil temperature in the model.

$$T_{f,out} = T_s - (T_s - T_{f,i})e^{\frac{-K_s L}{\dot{m}C_{p,f}}} \tag{4}$$

where α is the thermal diffusivity of the medium through which heat travels, $T_{f,out}$ is the fluid temperature exiting a pipe of length L (m). T_s is the surrounding soil temperature, $T_{f,i}$ is the initial water temperature entering the pipe, and K_s is the soil thermal conductivity ($Wm^{-1}{}^{\circ}C^{-1}$). $\dot{m}$ is the mass flow rate (Kgs^{-1}) and $C_{p,f}$ is the specific heat of the working fluid ($Jkg^{-1}\,{}^{\circ}C^{-1}$). Boundary and initial conditions for the solution domain are described as follows. Initial temperature distribution of the soil profile (T_i) was obtained from the Kusuda model, equation (5)[24]:

$$T_i = T(x, y), t = 0$$

$$\frac{\partial T}{\partial x} = 0, x = x_{max}$$

$$\frac{\partial T}{\partial x} = 0, x = 0$$

$$Q_t(W/m^2), y = 0$$

$$T(y, t) = T(y, t)_{Kusuda}, \ y = y_{max}$$

$$T(y, t)_{Kusuda} = T_{avg} + T_{amp}e^{-y\sqrt{\frac{\pi}{\alpha_s P}}} \cos(2\pi\frac{t}{P} - y\sqrt{\frac{\pi}{\alpha_s P}}) \tag{5}$$

where T_{avg} is the average annual surface temperature, T_{amp} is the amplitude of fluctuation of the annual surface temperature, y is the depth from ground surface (m), α_s is soil thermal diffusivity ($m^2 s^{-1}$), P is the duration of a year in seconds, and t is the time of the year in seconds.

Partial derivation of temperature in x-direction was written with a central difference scheme:

$$\frac{\partial^2 T}{\partial x^2}\Big|_{(i,j)}^n = \frac{T_{i-1,j}^n - 2T_{i,j}^n + T_{i+1,j}^n}{(\Delta x)^2} + O(\Delta x)^2$$

$$\approx \frac{T_{i-1,j}^n - 2T_{i,j}^n + T_{i+1,j}^n}{(\Delta x)^2} = \frac{\delta_x^2 T^n}{(\Delta x)^2} \tag{6}$$

where:

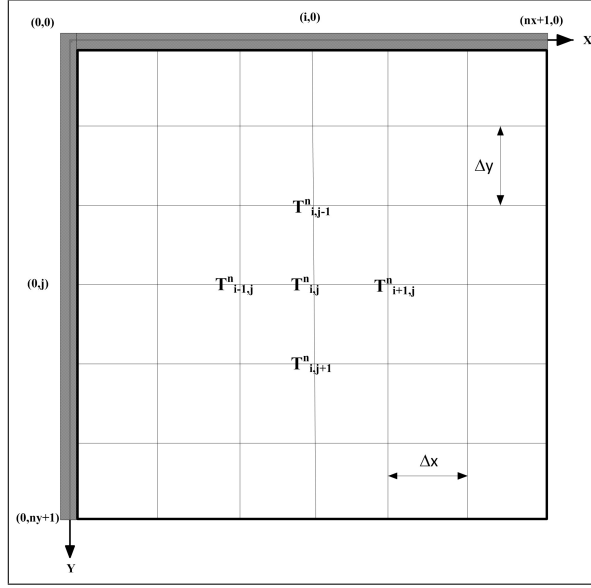$$\delta_x^2 T = T_{i-1,j} - 2T_{i,j} + T_{i+1,j} \tag{7}$$

Figure 3: Two dimensional grid of solution domain [12]

Using the same discretization for y-direction, the governing heat equation therefore can be expressed in terms of nodal temperature values in its explicit form as in equation (8). Next, a scheme was selected to march through time. As depicted in Figure 3, the solution domain was discretized in $n_x + 1$ nodes in x and $n_y + 1$ nodes in the y-direction, of which inner domain was used to solve for the temperature distribution of each cross section of the physical domain. The nodes on the boundary were separated to force boundary conditions in x and y direction.

$$\frac{T^{n+1} - T^n}{\Delta t} = \alpha [\frac{\delta_x^2 T^n}{(\Delta x)^2} + \frac{\delta_y^2 T^n}{(\Delta y)^2}] \tag{8}$$

A fully explicit finite difference solution scheme was employed to solve for temperature distribution of the solution domain. The model was constructed in MATLAB. Time steps of 1800 seconds and space discretization of $\Delta x = \Delta y = 0.1\ m$ were chosen based on a stability analysis of the model undertaken in the author's previous work [12].

Fully explicit finite difference formulation of the heat conduction equation takes the form of equation (9).

$$T_{i,j}^{n+1} - T_{i,j}^n = r(T_{i-1,j}^n - 2T_{i,j}^n + T_{i+1,j}^n) + r(T_{i,j-1}^n - 2T_{i,j}^n + T_{i,j+1}^n) \tag{9}$$

where:

$$r_x = \frac{\alpha \Delta t}{(\Delta x)^2} \ , \ r_y = \frac{\alpha \Delta t}{(\Delta y)^2} \ , \ r_x = r_y = r \tag{10}$$

Rearranged form of the explicit equation will take the form of equation (11):

8

$$T^{n+1} = rT^n_{i-1,j} + rT^n_{i+1,j} + rT^n_{i,j-1} + rT^n_{i,j+1} + (1-4r)T^n_{i,j} \tag{11}$$

Once the homogeneous case formulation was performed, the next step was adjustments to the difference equations to take into account the effects of the internal boundary conditions on the top and bottom of the intermediate layer. To meet the temperature and flux conditions on the internal boundaries, the energy balance on the interfacial nodes of intermediate layer and soil was obtained by writing the nodal fluxes and the energy storage term for the control volume around each node. Figure 4 depicts the energy balance for a node on the top and bottom of the intermediate layer interface, the control volume around the node, and the heat fluxes involved. The resulting energy balance is shown in the equation (12):

$$q_1 + q_3 - q_2 - q_4 = (\rho C_p)_{avg} \cdot \Delta x \cdot \Delta y \frac{\partial T_{i,j}}{\partial t}, \tag{12}$$

where:

$$(\rho C_p)_{avg} = \frac{(\rho C_p)_s + (\rho C_p)_{TDA}}{2} \quad , \quad K_{avg} = \frac{K_s + K_{TDA}}{2}$$

Figure 4: The intermediate (TDA) layer top and bottom interfaces energy balance [12]

and the values of heat fluxes are:

$$q_1 = K_{avg} \cdot \frac{T^n_{i-1,j} - T^n_{i,j}}{\Delta x} \cdot \Delta y \tag{13}$$

$$q_2 = K_{avg} \cdot \frac{T^n_{i+1,j} - T^n_{i,j}}{\Delta x} \cdot \Delta y \tag{14}$$

$$q_3 = K_s \cdot \frac{T^n_{i,j-1} - T^n_{i,j}}{\Delta y} \cdot \Delta x \tag{15}$$

$$q_4 = K_{TDA} \cdot \frac{T^n_{i,j+1} - T^n_{i,j}}{\Delta y} \cdot \Delta x \tag{16}$$

9

Substituting the flux equations into the energy balance equation and rearranging the equations results in the introduction of new parameters in the difference equation as described below.

$$r_{avg} = \frac{K_{avg}}{(\rho C_p)_{avg}} \cdot \frac{\Delta t}{(\Delta x)^2}, \; r_{TDA} = \frac{K_{TDA}}{(\rho C_p)_{avg}} \cdot \frac{\Delta t}{(\Delta x)^2}, \; r_s = \frac{K_s}{(\rho C_p)_{avg}} \cdot \frac{\Delta t}{(\Delta x)^2} \tag{17}$$

The difference formulas obtained previously for the explicit method were revised to account for the heat flux through the TDA top and bottom layers resulting in the equations (18) and (19).
TDA top layer:

$$T^{n+1} = r_{avg}T_{i-1,j}^n + r_{avg}T_{i+1,j}^n + r_S T_{i,j-1}^n + r_T T_{i,j+1}^n + (1 - 2r_{avg} - r_S - r_T)T_{i,j}^n \tag{18}$$

TDA bottom layer:

$$T^{n+1} = r_{avg}T_{i-1,j}^n + r_{avg}T_{i+1,j}^n + r_T T_{i,j-1}^n + r_S T_{i,j+1}^n + (1 - 2r_{avg} - r_S - r_T)T_{i,j}^n \tag{19}$$

4. Genetic algorithm

The idea of utilization of Genetic Algorithm (GA) in engineering applications was inspired by natural selection. This selection represents the concept of the higher survival chance of the fittest individual in its environment through successive generations to find the optimal design parameters among the others. More information about GA optimization can be found in [25]. The main advantages of GA over traditional optimization algorithms are that it does not require and does not depend on gradient information of the objective function; instead it uses a population of design points and randomly utilizes information from each generation to the subsequent one; and, there is a potential to make the population converge to the Pareto-optimal set. The latter property is a crucial appeal of GA in multi-objective optimization problems that enables us to use GA in combination with a Pareto-set filter [26] to obtain a near approximation of the entire set of non-dominated solutions. The specifications of the GA implementation in the present study are listed in Table 2.

Table 2: Gaoptimset options used in the analysis

PopulationSize	500	**CreationFcn**	@gacreationuniform
Generations	50	**FitnessScalingFcn**	@fitscalingprop
PopulationType	doubleVector	**SelectionFcn**	@selectiontournament
EliteCount	2	**CrossoverFcn**	@crossoversinglepoint
CrossoverFraction	0.7	**MutationFcn**	(@mutationuniform,.02)
MigrationDirection	forward	**Display**	'iter'
MigrationInterval	15	**UseParallel**	'always'
MigrationFraction	0.1		

Given the complex nature of the relationships between a GSHP unit, designers often should heavily rely on their level of experience to select the best heat pump design. Even with a huge deal of experience, these designs are

potentially distant from the required heating loads of a building due to the common practice peak load design criteria. Several researchers in the heat transfer literature have come to the conclusion that optimization schemes can benefit the design process where the effects of the climatic conditions is to be closely considered in an efficient design process [27, 28, 29, 30, 31, 32]. In their comprehensive work on vertical [30] and horizontal [31] ground source heat pumps, Sanaye modeled the thermodynamic cycle of the heat pump in conjunction with the thermal resistance pipe model to obtain the optimized operational parameters. Sayyaadi does a similar study via exergy analysis of a vertical ground source heat pump [32]. Authors of this paper are specifically concerned with the effects of the climatic conditions on the selection of the optimized operational parameters for a horizontal GSHP in the presence of a non-homogeneous soil profile. The optimization algorithm is supposed to provide the designers of the system with beneficial information regarding the ground pipe design where the absence of the experience can cause a wide deviation from the optimized cost and operation path.

To evaluate the potential benefits of the intermediate layer in different climate conditions, three cities across the nation were selected in order to perform the optimization analysis. Buffalo's climate condition requires space heating for majority of the year (550 cooling-degree-days), so Buffalo was assumed the heating dominated city with eight months heating (starting on October) to be representative of the cold climate. Miami case (4383 cooling-degree-days) was analyzed for pure conditioning to represent the warm climate. Simulation for Dallas was done with the assumption of six month heating (November-April with cooling-degree-days less than 150) to be the representative of a mild climate condition. To simplify the introduction of the weather data, the air and dew-pint temperature, and solar radiation values for these cities were introduced to the model via estimation of these inputs by cosine functions (equations 20, 21, and 22). Weather data were obtained form the National Operational Hydrologic Remote Sensing Center (NOHRSC) and curve-fitting was undertaken in Microsoft Excel environment to obtain the input parameters to the cosine models. A summary of the input parameters to the model for these cities is presented in table 3.

Table 3: Weather data for selected cities as input to the model

City	Buffalo	Dallas	Miami
T_{a-avg} (°C)	9.3	19.7	23.7
T_{a-amp} (°C)	14.1	12.2	6.8
α_{air} (month)	10.1	10.1	10.3
$T_{dew-avg}$ (°C)	4.3	9.4	18.1
$T_{dew-amp}$ (°C)	12.2	11.6	7.3
α_{dew} (month)	10.2	10	10.4
Q_{si-avg} (Wm^{-2})	142	168	182
Q_{si-amp} (Wm^{-2})	75	59	33
$\alpha_{Q_{si}}$ (month)	9.2	10.2	10.1
U_s (ms^{-1})	4.2	4.1	4

$$T_{air} = T_{a-avg} + T_{a-amp} \cos(2\pi \frac{t}{P} - \frac{\alpha_{air}}{12}) \tag{20}$$

where T_{a-avg} is the average annual air temperature, T_{a-amp} is the amplitude of fluctuation of annual air temperature, and α_{air} is the fitted cosine model phase difference for air temperature, calculated based on the start time of the modeling on October first (the assumed heating season start time).

$$T_{dewpoint} = T_{dew-avg} + T_{dew-amp} \cos(2\pi\frac{t}{P} - \frac{\alpha_{dew}}{12}) \tag{21}$$

where $T_{dew-avg}$ is the average annual dew-point temperature, $T_{dew-amp}$ is the amplitude of annual dew-point temperature variation, and α_{dew} is the fitted cosine model phase difference for dew-point temperature.

$$Q_{si} = Q_{si-avg} + Q_{si-amp} \cos(2\pi\frac{t}{P} - \frac{\alpha_{Q_{si}}}{12}) \tag{22}$$

where Q_{si-avg} is the average annual solar radiation reaching the surface, Q_{si-amp} is the amplitude of fluctuation of the solar radiation throughout the year, and the $\alpha_{Q_{si}}$ is the fitted cosine model phase difference for radiation.

A genetic algorithm (GA) optimization scheme was designed to obtain the optimum values of the intermediate layer configuration (thickness and position), working fluid type, and inlet fluid temperature ranges. The results of the simulation will provide insights on the benefits of introduction of an intermediate layer on the performance of a GSHP throughout the year. The model outputs will clarify what are the optimal properties and configuration of the intermediate layer and what are the optimal entering water temperatures to the ground throughout the year to achieve the maximal efficiency. The ultimate motivation behind the analysis is to determine whether the operating parameters for different months of the year are in a range that confirms the benefits of utilization of a capacity control strategy or a set of selected operational parameters can be used for all months without deviating from the optimized condition.

Table 4: Working fluid properties

Index number	Fluid	Thermal conductivity $(Wm^{-1\circ}C^{-1})$	Specific heat $(JKg^{-1\circ}C^{-1})$	Density (Kgm^{-3})	Dynamic viscosity $(Kgm^{-1}s^{-1}) \cdot 10^{-3}$
1	Water	0.6	4183	998.3	1
2	6 % Propylene-glycol and water	0.476	4140	1010	1.5
3	13 % Propylene-glycol and water	0.432	4100	1010	1.9
4	18 % Propylene-glycol and water	0.408	4060	1020	3
5	24 % Propylene-glycol and water	0.389	4020	1020	6.3

Seven input variables (decision variables) were chosen to feed the core finite difference model in each run of the GA. These inputs comprise working fluid properties, minimum, mean and maximum entering water temperature values, the intermediate layer thickness, position and thermal properties. To let the evolutionary algorithm search in a broader spectrum of potential answers, the algorithm was allowed to choose between a range of practical working fluid properties (table 4, extracted from the IGSHPA guideline [1]) and also a range of common soil properties in ground heat pump works (table 5, extracted from the manual for the soil and rock classification for design of ground heat pumps [21]).

The values of heat extraction/dissipation rates were calculated based on equation (23) for each run after selection of these parameters. The time averaged values of outlet (T_{out}^{avg}) and inlet (T_{in}^{avg}) working fluid temperatures for the simulation period (monthly or seasonal) are used to calculate energy extraction/dissipation rates in heating/cooling modes. The heat pump work was calculated based on the friction factor and Reynolds number described in [33]. The objective function used in the simulation is equal to the reciprocal of difference between the energy extraction rate and the circulating pump energy consumption rate. A single-objective genetic algorithm model was used subsequently to

search for the parameters that minimize the objective function or, in other words, maximize the net energy extraction/dissipation rates. It was assumed that maximum heating/cooling energy demand from the ground pipes does not exceed 1.5 Kw in any of the cities while the optimization was aimed towards maximizing the extraction/dissipation rates. A population size of 500 and 50 generation was selected for each run of the model. A total number of 32 processors of 48 GB memory were used for each monthly run of the model which resulted in runtime of about 7 hours. A total number of 64 processors of 48 GB memory were used for each annual run which resulted in the runtime of about 65 hours for each year.

$$Energy = \dot{m} \cdot C_{p,f} \cdot (T_{out}^{avg} - T_{in}^{avg}) \tag{23}$$

Table 5: Intermediate layer thermal properties

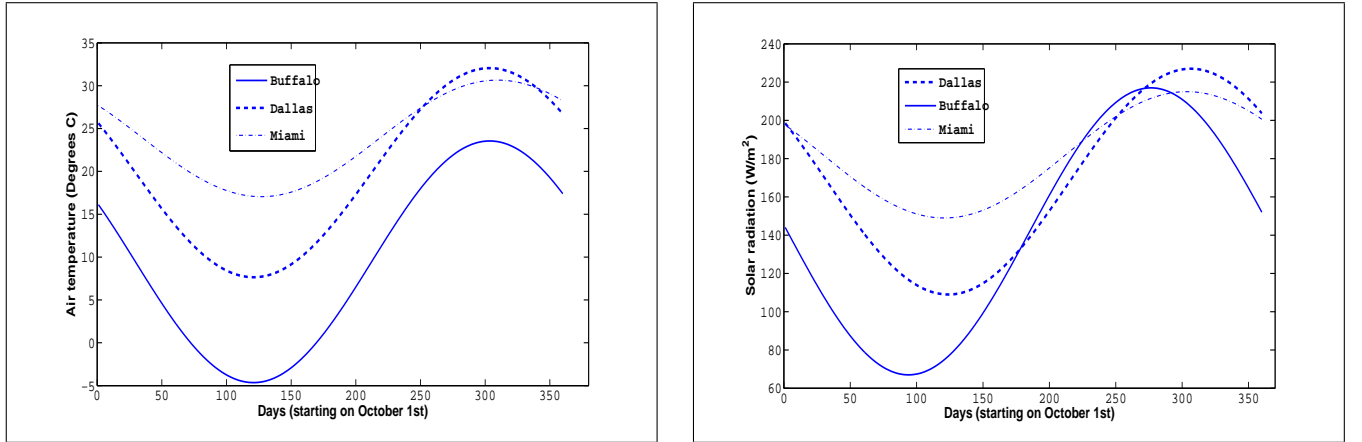| Index number	Intermediate material	Thermal conductivity $(Wm^{-1\circ}C^{-1})$	Thermal diffusivity $(cm^2 s^{-1})10^{-8}$
1	TDA	0.29	58
2	Sand	0.77	45
3	Clay	1.11	54
4	Loam	0.91	49
5	Saturated silt or clay	1.67	66
6	Saturated sand	2.5	93

Figure 5: Annual air and solar radiation variation in the selected cities

5. Results and discussion

The optimized monthly parameters for three cities are presented in tables 6 to 8. The main motive behind doing the optimization separately for each month was to have an estimate of what the range of the optimal operating parameters are and how the optimal parameters vary from month to month. The selection of the intermediate layer material type by the algorithm assures a non-homogeneous profile that provides the best performance. It seems from the results that TDA blanket demonstrates more benefits in certain climate conditions and within each climate also its potential

advantage is more highlighted in some months more than others. Results for Buffalo (table 6) show that TDA is selected as the dominant intermediate layer for eight months of the year of which five months are in heating season. In the cooling season, TDA was not selected only in July where the saturated clay tends to exhibit a dominant effect as an intermediate layer.

Table 6: GA results for Buffalo

Month	Fluid (index)	EWT_{min} (°C)	EWT_{max} (°C)	EWT_{mean} (°C)	Thickness (m)	Position (m)	Intermediate material	Energy (Watt)	%
Oct	3	4.0		5.2	0.4	1.4	Saturated clay	558	6.5
Nov	1	-3.0		5.2	0.7	0.6	TDA	492	4.7
Dec	2	-3.0		5.5	0.9	0.5	TDA	515	13.2
Jan	2	-3.0		8.0	1.0	0.5	TDA	474	18.8
Feb	2	-3.0		6.8	1.0	0.7	TDA	375	19.4
Mar	1	-3.0		5.2	0.5	1.0	TDA	252	6.8
Apr	3	-2.6		5.2	0.8	1.0	Saturated clay	179	9.1
May	3	4.7		5.2	0.4	1.3	Saturated Clay	295	11.7
Jun	1		40.4	35.8	0.5	0.5	TDA	1500	2.5
Jul	2		42.4	32.5	0.3	1.4	Saturated Clay	1500	1.2
Aug	4		43.0	41.6	0.3	1.0	TDA	1500	1.2
Sep	4		45.6	34.5	0.4	0.5	TDA	1500	1.3
Avg. Heating		-1		5.9	0.7	0.8		393	
Avg. Cooling			42.8	36.1	0.4	0.8		1500	

The results for Dallas (table 7) on the other hand show a different trend where TDA has been selected as the dominant intermediate layer mostly in warmer months of the year whereas the colder months where saturated clay yields the optimal efficiency. The reason behind this observation probably lies in the difference in the phase change angle of the annual temperature and solar radiation for Buffalo and Dallas. The maximum and minimum ambient temperature and solar radiations occur with a time lag for these cities (Figure 5) where the interplay of energy exchange processes on the surface seems to favor the most conductive intermediate layer versus the least conductive layer or vice versa in certain months of the year.

TDA was selected by the algorithm in hottest months of the year in Miami (table 8) to yield the highest energy dissipation rates. One interesting observation from the monthly results is that only the two intermediate material with lowest and highest thermal conductivities were selected as the choice blanket material through the optimization algorithm. The fact that TDA (the least conductive) or saturated clay (the most conductive) were selected among the provided list of intermediate material suggests that the ground pipes can benefit from a blanket above the pipe burial depth throughout the year but not necessarily from the one with highest insulation properties. An energy weighted average value of the operating parameters for heating and cooling seasons in selected cities is also provided at the end of each table for the sake of comparison between cities.

It should be noted that this modeling procedure do not take into account other characteristics of either of the TDA or saturated clay materials. Characteristics such as the porosity and water holding capacity which might poten-

Table 7: GA results for Dallas

Month	Fluid (index)	EWT_{min} (°C)	EWT_{max} (°C)	EWT_{mean} (°C)	Thickness (m)	Position (m)	Intermediate material	Energy (Watt)	%
Oct	1		59.0	43.2	0.2	0.5	TDA	1500	0.2
Nov	2	-3.0		5.2	0.4	1.2	Saturated clay	1071	4.9
Dec	5	-3.0		5.2	0.7	1.1	Saturated clay	1096	1.7
Jan	4	-3.0		5.2	1.0	0.1	TDA	1054	0.1
Feb	2	-3.0		7.1	0.5	1.3	Saturated clay	1017	4.9
Mar	1	-3.0		5.2	0.9	0.8	Saturated clay	937	6.8
Apr	1	-2.1		5.2	0.4	1.5	Saturated clay	825	6.7
May	1		53.6	41.4	0.2	1.0	TDA	1500	0.3
Jun	3		53.4	36.2	0.2	0.7	TDA	1500	1.7
Jul	1		51.8	29.5	0.5	0.8	TDA	1500	1.7
Aug	4		51.6	46.9	0.5	0.9	TDA	1500	0.9
Sep	3		56.6	35.1	0.2	0.1	TDA	1500	1.7
Avg. Heating		-2.9		5.5	0.7	1		1000	
Avg. Cooling			54.3	38.7	0.3	0.7		1500	

tially contribute to considerably different performance results than that only based on the heat conduction in the soil medium. TDA's porous structure can potentially enhance the moisture migration to the underlying layers of soil where higher moisture can contribute to higher thermal conductivities of the soil around the pipes. It is expected that this characteristics of TDA has a more substantial effect in the summer time specially in regions with less rainfall events. Authors are currently in the process of installation of a field experiment with TDA blanket and a control clayey section to verify other potential enhancements on GSHP performance by utilization of the TDA layer.

A comparison between the working fluid minimum and average temperatures for the heating season in Buffalo and Dallas shows that relatively similar ranges are selected by the algorithm for optimal operation in cold season. On the other hand, as expected, the optimized maximum and minimum fluid temperatures in summer are comparatively higher for Miami and Dallas than corresponding values for Buffalo to ensure the highest energy dissipation to the ground.

The values in the last column in tables 6 to 8 represent the percentage energy extraction/dissipation rate increase compared to the homogenous soil profile in different months. There are trends in comparing the results for similar seasons in different cities. The percentages increase in energy extraction rate for the coldest months in Buffalo (Jan-Feb) are as high as 18-19 % as compared to similar time periods for Dallas with highest values of 5-6 %. This finding can be translated in the potential for higher efficiency achievement with a non-homogeneous soil profile in heating season with more pronounced effects in colder climates (Buffalo). It should be noted again that the material choice for the intermediate layer in the cold season in Buffalo is TDA versus the saturated clay for Dallas.

A similar comparison for the cooling season in all cities reveals an interesting observation. The highest efficiency improvements for cooling in Miami happen to be in the coldest month of the year with increase in energy dissipation rates of approximately 6-8 %. The optimization algorithm tends to choose higher working fluid temperatures, com-

Month	Fluid (index)	EWT_{min} (°C)	EWT_{max} (°C)	EWT_{mean} (°C)	Thickness (m)	Position (m)	Intermediate material	Energy (Watt)	%
Oct	2		59.6	44.6	0.6	1.2	Saturated Clay	1499	2.2
Nov	3		72.4	54.6	0.3	0.3	Saturated Clay	1500	0.1
Dec	2		79.8	69.6	0.7	1.0	Saturated Clay	1359	7.1
Jan	1		67.3	67.3	0.8	1.1	Saturated Clay	712	7.4
Feb	1		80.0	69.2	0.8	1.0	Saturated Clay	649	6.2
Mar	1		80.0	69.2	0.9	1.0	Saturated Clay	1145	8.5
Apr	4		66.7	66.0	0.6	1.0	Saturated Clay	1500	0.6
May	1		57.5	44.6	0.5	0.1	TDA	1500	1.1
Jun	2		51.6	50.3	0.5	0.7	TDA	1500	0.2
Jul	3		52.2	51.3	0.1	0.3	TDA	1500	0.9
Aug	3		52.7	43.1	0.5	0.1	TDA	1500	0.6
Sep	1		53.7	51.7	0.3	0.1	TDA	1500	0.3
Avg. Cooling			63	55.2	0.5	0.6		1322	

pared to the warmer months, with the highest intermediate layer conductivity (saturated clay) to maximize the heat flux to the ground and subsequently increase the efficiency. This trend does not repeat itself in warmer months as the algorithm searches through the large population of possible solutions. The comparison for the cooling season in all cities shows that relatively small efficiency improvements are achievable with the non-homogeneous soil profile for cooling purposes in warmer months of the year. It should be noted that the performance of the homogeneous system is very close to the maximum expected cooling capacity (1500 Watts) in warmest months of the year for all of these cities which contributes to the marginal improvements with a non-homogeneous soil profile. In other words, if the designed ground pipe network was supposed to provide higher energy rates, the percentage increase in energy extraction rates would probably be higher and more pronounced with the non-homogeneous soil profile. It would be safe to state that if chosen to use a non-homogeneous soil profile for cooling-only purposes in a warm climate, a high conductive intermediate layer can be more beneficial in coldest months of the year.

After performing the analysis for each month and gaining adequate knowledge of the relationship between selected variables, the next step of the modeling was focused on finding the optimal values of the inlet fluid temperature and the configuration of the intermediate layer year-round. Knowing what the two dominant choices of the algorithm for the intermediate blanket are, separate runs of the model with TDA were executed to compare the results with the homogeneous and saturated clay soil profiles. The working fluid properties was set to 13 % Propylene-glycol and water mixture for all the annual runs. The existing knowledge of the system from monthly results helped constructing a more efficient optimization scheme with less variables for the annual runs. The goal for this step was to obtain the optimal values of temperatures and intermediate layer configuration by optimizing the energy extraction/dissipation for the whole year. This approach provides the designer with the optimized working fluid temperatures and intermediate layer's configuration which yields the best performance.

The results of annual runs are presented in tables 9 to 11. The percentages in the table refer to the percent increase

in the energy extraction/dissipation rates compared to the homogeneous soil profile. The obtained optimized temperature values and intermediate layer configuration for TDA were used to run the homogeneous and saturated clay scenarios for the sake of comparison. For the Buffalo case, the algorithm yields higher maximum and average temperature values for heating season compared to average monthly values (Table 6) to obtain the maximum performance over the entire season. A similar trend was observed for Dallas with higher mean working fluid temperature in heating season compared to average monthly values (Table 7). The working fluid temperature values are comparatively lower for Buffalo than Dallas for annual results. The optimized annual TDA thickness and positions are relatively smaller than the values obtained in the monthly optimization. The average annual attainable energy rates are also consistently lower for the annual runs compared to monthly values.

Table 9: Annual results for Buffalo

EWT_{min} (°C)	$EWT_{mean-heating}$ (°C)	Thickness (m)	Position (m)	EWT_{max} (°C)	$EWT_{mean-cooling}$ (°C)
-2.3	7.0	0.5	0.3	45.7	31.7
TDA energy (Watt)	Clay energy (Watt)	Homogeneous energy (Watt)	Mode	% TDA	% Clay
324	274	280	Heating	15.7	-2.1
1497	1375	1391	Cooling	7.6	-1.2

Table 10: Annual results for Dallas

EWT_{min} (°C)	$EWT_{mean-heating}$ (°C)	Thickness (m)	Position (m)	EWT_{max} (°C)	$EWT_{mean-cooling}$ (°C)
-2.7	23.5	0.5	0.4	52.6	29.6
TDA energy (Watt)	Clay energy (Watt)	Homogeneous energy (Watt)	Mode	% TDA	% Clay
635	608	612	Heating	3.8	-0.7
1431	1378	1382	Cooling	3.5	-0.3

Table 11: Annual results for Miami

EWT_{min} (°C)	$EWT_{mean-heating}$ (°C)	Thickness (m)	Position (m)	EWT_{max} (°C)	$EWT_{mean-cooling}$ (°C)
		0.8	0.4	73.0	55.0
TDA energy (Watt)	Clay energy (Watt)	Homogeneous energy (Watt)	Mode	% TDA	% Clay
1298.0	1482.0	1456.0	Cooling	-10.9	1.8

The values of the annual energy rates with TDA and saturated clay compared to the homogeneous case suggest considerably lower annual performance with clay for both heating and cooling season in Buffalo and Dallas (Tables 9 and 10). The results for Buffalo are in the order of 1-2 % worse than the homogeneous case with clay. The similar comparison for Dallas shows nearly identical annual performance with clay as the homogeneous case. TDA exhibits

higher performance in heating than cooling (15.7 versus 7.6), and comparatively higher increase in energy rates for Buffalo than Dallas in heating (15.6 versus 3.8). The results for Miami on the other hand suggest a significantly better performance with clay layer than TDA (1.8 % versus -10.9 %) for cooling. Although, the value of annual increase in energy dissipation rate (1.8 %) with clay is considerably lower than the monthly values obtained for Miami (Table 8).

The comparison between the optimized annual heating/cooling energy rates with the monthly values shows that the optimization algorithm yields values that stray from the optimized monthly values. This is because of the fact that it is more challenging for the algorithm to find operational parameters which level off the difference between seasonal energy rates and highest achievable monthly values. This causes the annual energy rates to be relatively lower than the ones attainable if the monthly control on the operating parameters (working fluid temperatures and intermediate layer configuration) was an option. These findings suggest that utilization of control strategies which allow the heat pump's functionality with variable working fluid temperatures (or variable refrigerant flow schemes) in different seasons can improve the overall performance of the GSHP.

6. Conclusions

Performance of a GHSP system with a non-homogeneous soil profile was examined via GA optimization algorithm. The evolutionary algorithm was given a range of working fluid properties, intermediate layer thermal properties, a range of operating temperatures, and the intermediate layer configuration to search for the optimized condition of the system. The optimization process was performed for three cities representing a cold (Buffalo), moderate (Dallas) and warm (Mmiami) climate for the sake of comparison. A summary of findings are listed below:

- A generic non-homogeneous soil profile showed the potential for significant GSHP performance improvement

- TDA demonstrated higher benefits in colder climate and with higher magnitudes in heating season

- TDA demonstrated marginal enhancement in cooling due to insignificant capacity difference than homogeneous scenario

- Saturated clay demonstrated potential for efficiency improvement in cooling for colder months in a relatively warm climate

- The annual optimized energy rates are lower than monthly values suggesting the necessity of a monthly operation control strategy

Despite different performance achievements with either a low conductance (TDA) or a high conductance (saturated clay) intermediate layer, a non-homogenous soil profile demonstrated the potential for increasing the the GSHPs performance. A shift in perspective toward control strategies for GSHPs from only the heat pump side to the ground pipe side of the system is suggested based on the model results. Further investigation of other attributes of a layered system which can potentially enhance the GSHP's performance is still required. TDA for example has a very porous structure enabling the water passage through the intermediate blanket. This characteristics of TDA has the potential to increase the thermal conductivity of the underlying soil by increasing the soil moisture content. Further investigation of the findings is planned through a field demonstration recently built on the University at Buffalo properties.

Acknowledgments

References

[1] IGSHPA, Ground source heat pump residential and light commercial design and installation guide, International Ground Source Heat Pump Association, Oklahama State University, Division of Engineering Technology, 2009.

[2] O. Zogou, A. Stamatelos, Optimization of thermal performance of a building with ground source heat pump system, Energy conversion and management 48 (2007) 2853–2863.

[3] H. Madani, J. Claesson, P. Lundqvist, Capacity control in ground source heat pump systems part II: Comparative analysis between on/off controlled and variable capacity systems, International Journal of Refrigeration 34 (2011) 1934–1942.

[4] T. Qureshi, Variable-speed capacity control in refrigeration systems, Applied Thermal Engineering 16 (1996) 103–113.

[5] H. Madani, J. Claesson, P. Lundqvist, Capacity control in ground source heat pump systems: Part I: modeling and simulation, International Journal of Refrigeration 34 (2011) 1338–1347.

[6] J. A. Shonder, Selecting the Design Entering Water Temperature for Vertical. Geothermal Heat Pumps in Cooling-Dominated Applications., ASHRAE Annual Meeting (2001) 16p.

[7] O. Siddiqui, A. Fung, H. Tse, D. Zhang, Modelling of the net zero energy town house in toronto using trnsys, and an analysis of the impact using thermal mass, in: 2008 Proceedings of the 2nd International Conference on Energy Sustainability, ES 2008, volume 2, Jacksonville, FL, United states, pp. 297–304.

[8] F. Conlin, W. S. Johnson, S. Wix, A TRNSYS/GROCS Simulation of a Horizontal Coil Ground-Coupled Heat Pump, Journal of Solar Energy Engineering 108 (1986) 185–191.

[9] C. Lee, Dynamic performance of ground-source heat pumps fitted with frequency inverters for part-load control, Applied Energy 87 (2010) 3507–3513.

[10] E. Kjellsson, G. Hellström, B. Perers, Optimization of systems with the combination of ground-source heat pump and solar collectors in dwellings, Energy 35 (2010) 2667–2673.

[11] R. G. Kapadia, S. Jain, R. S. Agarwal, Transient characteristics of split air-conditioning systems using R-22 and R-410A as refrigerants, HVAC and R Research 15 (2009) 617–649.

[12] A. Rezaei B., E. M. Kolahdouz, G. F. Dargush, A. S. Weber, Ground source heat pump pipe performance with Tire Derived Aggregate, International Journal of Heat and Mass Transfer 55 (2012) 2844–2853.

[13] J. Shao, J. Zarling, Thermal conductivity of recycled tire rubber to be used as insulating fill beneath roadways, Technical Report, Institute of Northern Engineering, University of Alaska Fairbanks, Fairbanks, 1995.

[14] B. Lawrence, D. Humphrey, L.-H. Chen, Field Trial of Tire Shreds as Insulation for Paved Roads, in: Cold Regions Engineering@ sPutting Research into Practice, ASCE, 1999, pp. 428–439.

[15] D. Humphrey, Tire Shreds as Lightweight Fill for Retaining WallsResults of Full Scale Field Trials, International Workshop on Lightweight Geomaterials, (2002) 261–268.

[16] H. Moo-young, K. Sellasie, D. Zeroka, G. Sabnis, Physical and Chemical Properties of Recycled Tire Shreds for Use in Construction, Journal of Environmental Engineering (2003) 921–929.

[17] D. Humphrey, A. Fiske, R. Eaton, Backcalculation of Thermal Conductivity of Tire Chips from Instrumented Test Section, Transportation Research Board 81st Annual Meeting (2002).

[18] H. L. Wappett, J. G. Zornberg, Full Scale Monitoring for Assessment of Exothermal Reactions in Waste Tires Final Report, Technical Report 27, Recycled Materials Resource Center, Project No . 27, University of Texas, Austin, 2006.

[19] F. Ling, T. Zhang, A numerical model for surface energy balance and thermal regime of the active layer and permafrost containing unfrozen water, Cold Regions Science and Technology 38 (2004) 1–15.

[20] G. E. Liston, D. K. Hall, An energy-balance model of lake-ice evolution, Journal of Glaciology 41 (1995) 373–382.

[21] J. Bose, Soil and rock classification for the design of ground-coupled heat pump systems-field manual, Electric Power Research Institute Special Report, EPRI CU-6600 (1989).

[22] H. Demir, A. Koyun, S. O. Atayilmaz, Determination of Optimum Design Parameters of Horizontal Parallel Pipe and Vertical U-Tube Ground Heat Exchangers, ASME Conference Proceedings (2009) 621–627.

[23] A. Koyun, H. Demir, Z. Torun, Experimental study of heat transfer of buried finned pipe for ground source heat pump applications, International Communications in Heat and Mass Transfer 36 (2009) 739–743.

[24] T. Kusuda, P. R. Achenbach, Earth Temperature and Thermal Diffusivity at Selected Stations in the United States, Technical Report, National Bureau of Standards Washington D C, 1965.

[25] D. Goldberg, Genetic Algorithms in Search; Optimization and Machine Learning, Addison-Wesley, Massachusetts, 1989.

[26] L. D. Cheng FY, Multiobjectve optimization design with Pareto genetic algorithm., Journal of Structural Engineering 123 (1997) 1252–1261.

[27] B. I. Kilkis, An Exergy Aware Optimization and Control Algorithm for Sustainable Buildings, International Journal of Green Energy 1 (2004) 65–77.

[28] J. Lohan, N. Burke, M. Greene, Climate variables that influence the thermal performance of horizontal collector ground source heat pumps BT, in: 8th Biennial ASME Conference on Engineering Systems Design and Analysis, volume 2006 of *Proceedings of 8th Biennial ASME Conference on Engineering Systems Design and Analysis, ESDA2006*, American Society of Mechanical Engineers, Department of Mechanical and Industrial Engineering, Galway-Mayo Institute of Technology, Dublin Road, Galway, Ireland, 2006.

[29] A. Pertzborn, G. Nellis, S. Klein, Impact of weather variation on ground-source heat pump design, HVAC&R Research 17 (2011) 174–185.

[30] S. Sanaye, B. Niroomand, Thermal-economic modeling and optimization of vertical ground-coupled heat pump, Energy Conversion and Management 50 (2009) 1136–1147.

[31] S. Sanaye, B. Niroomand, Horizontal ground coupled heat pump: Thermal-economic modeling and optimization, Energy Conversion and Management 51 (2010) 2600–2612.

[32] H. Sayyaadi, E. Amlashi, Multi-objective optimization of a vertical ground source heat pump using evolutionary algorithm, Energy Conversion and 50 (2009) 2035–2046.

[33] L. S, Kakac; H., Heat exchangers: selection, rating and thermal design., CRC Press, 2nd ed. bo edition, 2002.